D_1-like dopamine receptors selectively block P/Q-type calcium channels to reduce glutamate release onto cholinergic basal forebrain neurones of immature rats

Toshihiko Momiyama[1,2] and Yugo Fukazawa[1]

[1]*Division of Cerebral Structure, National Institute for Physiological Sciences, Okazaki 444-8787, Japan*
[2]*Core Research for Evolutional Science and Technology (CREST), Japan Science and Technology Corporation, Kawaguchi, Japan*

Whole-cell patch-clamp recordings of non-NMDA glutamatergic EPSCs were made from identified cholinergic neurones in slices of basal forebrain (BF) of young rats (P13–P18), to investigate the subtypes of calcium channels involved in dopamine D_1-like receptor-mediated presynaptic inhibition of the EPSCs. The BF cholinergic neurones were pre-labelled by intracerebroventricular injection of a fluorescent marker, Cy3-192IgG. A D_1-like receptor agonist, SKF 81297 (30 μM) suppressed the EPSCs reversibly by about 30%, and this inhibition was reproducible. Calcium channel subtypes involved in the glutamatergic transmission were elucidated using selective Ca^{2+} channel blockers. The N-type Ca^{2+} channel blocker ω-conotoxin (ω-CgTX, 3 μM) suppressed the EPSCs by 57.5%, whereas the P/Q-type channel selective blocker ω-agatoxin-TK (ω-Aga-TK, 200 nM) suppressed the EPSCs by 68.9%. Simultaneous application of both blockers suppressed the EPSCs by 96.1%. The R-type Ca^{2+} channel blocker SNX-482 (300 nM) suppressed the EPSCs by 18.4%, whereas nifedipine, the L-type Ca^{2+} channel blocker (10 μM), had little effect. In the presence of ω-Aga-TK, SKF 81297, a dopamine D_1-like receptor agonist, had no effect on the EPSCs. On the other hand, SKF 81297 could still inhibit the EPSCs in the presence of either ω-CgTX, SNX-482 or nifedipine. SKF 81297 had no further effect on the EPSCs when external Ca^{2+} concentration was raised to 7.2 mM in the presence of ω-Aga-TK, but could still inhibit the EPSCs in high Ca^{2+} solution after ω-CgTX application. Forskolin (FK, 10 μM), an activator of adenylyl cyclase pathway, suppressed the EPSCs, and the FK-induced effect was mostly blocked in the presence of ω-Aga-TK but not that of ω-CgTX. These results suggest that D_1-like receptor activation selectively blocks P/Q-type calcium channels to reduce glutamate release onto BF cholinergic neurones.

(Resubmitted 28 November 2006; accepted after revision 11 January 2007; first published online 18 January 2007)
Corresponding author T. Momiyama: Division of Cerebral Structure, National Institute for Physiological Sciences, Okazaki 444-8787, Japan. Email: tmomi@nips.ac.jp

Basal forebrain (BF) nuclei, consisting of the vertical and horizontal limbs of diagonal band of Broca (HDBB), substantia innominata (SI) and nucleus of basalis (nB), form the principal source of cholinergic innervation to the cortical and subcortical brain regions (Rye *et al.* 1984). Pathologically, degeneration of these cholinergic neurones has been observed in patients with Alzheimer's disease (Coyle *et al.* 1983; Oyanagi *et al.* 1989). Morphological studies have shown that the BF region receives dopaminergic fibres from the ventral tegmental area, substantia nigra pars compacta and medial zona interna (Martinez-Murillo *et al.* 1988; Semba *et al.* 1988; Eaton *et al.* 1994). It has been electrophysiologically demonstrated that activation of presynaptic dopamine D_1-like receptors reduces glutamate release onto magnocellular BF neurones, mainly cholinergic, in a calcium-dependent manner (Momiyama *et al.* 1996). Although multiple types of Ca^{2+} channels including N-, P/Q- and R-type channels are involved in the fast synaptic transmission in the central nervous system (Luebke *et al.* 1993; Takahashi & Momiyama, 1993; Regehr & Mintz, 1994; Umemiya & Berger, 1994; Wheeler *et al.* 1994; Wu & Saggau, 1994; Wu *et al.* 1998), it remains to be elucidated whether activation of these D_1-like receptors blocks specific subtypes of Ca^{2+} channels. The aim of the present study is to identify which Ca^{2+}-channel subtypes are involved in the D_1-like receptor-mediated presynaptic inhibition of the non-NMDA glutamatergic transmission onto BF cholinergic neurones. In the present study, cholinergic BF neurones could be pre-labelled using Cy3-192IgG (Wu *et al.* 2000), a marker for p75 neurotrophic factor receptors (Hartig *et al.* 1998), as neurones

 DOI: 10.1113/jphysiol.2006.125724

expressing these receptors in the BF region are exclusively cholinergic (Batchelor *et al.* 1989; Sobreviela *et al.* 1994).

Methods

Intra-cerebroventricular injection of Cy3-192IgG and brain slice preparation

All experimental procedures were done according to the Guiding Principles for the Care and Use of Animals in the Field of Physiological Sciences of the Physiological Society of Japan (1998) and the UK Animals (Scientific Procedures) Act 1986. Rats (10- to 14-days-old) were anaesthetized with pentobarbital (50 mg kg^{-1} I.P.) and then mounted into a stereotaxic apparatus. Cy3-192IgG (3–4 μl; 0.4 mg ml^{-1}, dissolved in saline) was injected unilaterally into the lateral ventricle of the rat using a Hamilton syringe (22 gauge needle) at a rate of 0.5 μl min^{-1} (Wu *et al.* 2000; Momiyama & Zaborszky, 2006). The coordinates of the lateral ventricle used were 0.9–1.0 mm posterior from Bregma, 1.0–1.1 mm lateral from midline, and 3.8–4.0 mm below from the dura.

Three to six days following intracerebroventricular injection of Cy3-192IgG, rats were killed by decapitation under deep halothane anaesthesia, and coronal slices containing the BF regions, including the HDBB and SI, were cut (300 μm thick) using a microslicer (PRO7, Dosaka, Kyoto, Japan) in ice-cold oxygenated cutting Krebs solution of the following composition (mM): choline chloride, 120; KCl, 2.5; $CaCl_2$, 0.5; $MgCl_2$, 7; NaH_2PO_4, 1.25; $NaHCO_3$, 26; D-glucose, 15; ascorbic acid, 1.3. The slices were then transferred to a holding chamber containing standard Krebs solution of the following composition (mM): NaCl, 124; KCl, 3; $CaCl_2$, 2.4; $MgCl_2$, 1.2; NaH_2PO_4, 1; $NaHCO_3$, 26; D-glucose, 10; pH 7.4 when bubbled with 95% O_2–5% CO_2. Slices were incubated in the holding chamber at room temperature (21–26°C) for at least 1 h before recording.

Whole-cell recording and data analysis

For recording, a slice was transferred to the recording chamber, held submerged, and superfused with standard Krebs solution (bubbled with 95% O_2–5% CO_2) at a rate of 3–4 ml min^{-1}. Neurones within the HDBB or SI were visually identified with a 60 ×; water immersion objective attached to an upright microscope (BX50WI, Olympus Optics, Tokyo, Japan). Images were detected with a cooled CCD camera (CCD-300T-RC, Nippon roper, Japan) and displayed on a video monitor (LC-150M1, Sharp, Japan). Cy3-192IgG-labelled neurones were visualized using the appropriate fluorescence filter (U-MWIG3, Olympus Optics, Tokyo, Japan). Pipettes for whole-cell recordings were made from standard-walled borosilicate glass capillaries (1.5 mm outer diameter; Clark Electromedical, Reading, UK). For the analyses of membrane properties, voltage-clamp or current-clamp recordings were carried out using a potassium gluconate-based internal solution of the following composition (mM): potassium gluconate, 120; NaCl, 6; $CaCl_2$, 5; $MgCl_2$, 2; K-EGTA, 0.2; K-Hepes, 10; Mg-ATP, 2; Na-GTP, 0.3 (pH adjusted with 1 M KOH). For synaptic currents recordings, patch pipettes were filled with a CsCl-based internal solution of the following composition (mM): CsCl, 140; NaCl, 9; Cs-EGTA, 1; Cs-Hepes, 10, Mg-ATP, 2 (pH adjusted with 1 M CsOH). Whole-cell recordings were made from Cy3-192IgG-labelled neurones using a patch-clamp amplifier (Axopatch 200B, Axon Instruments, Foster City, CA, USA). The series resistance was measured from the amplifier, and the data were discarded if the series resistance changed by more than 10% of the initial value. The access resistance was monitored by measuring capacitative transients obtained in response to a hyperpolarizing voltage step (5 mV, 25 ms) from a holding potential of −65 mV. No correction was made for the liquid junction potentials (calculated to be 5.0 mV by pCLAMP7 software, Axon Instruments). Synaptic currents were evoked at a rate of 0.2 Hz (every 5 s) by extracellularly delivered voltage pulses (0.2–0.4 ms in duration) of suprathreshold intensity via a stimulating electrode filled with 1 M NaCl. Paired-pulse stimuli were delivered with an interstimulus interval of 50 ms. The stimulating electrode was placed within 50–120 μm radius of the recorded neurone. The position of the stimulating electrode was varied until a stable response was evoked in the recorded neurone. All the excitatory postsynaptic currents (EPSCs) were evoked at a holding potential of −65 mV. Experiments were carried out at room temperature (21–26°C).

Data were stored on digital audio tapes using a DAT recorder (SONY, Japan; DC to 10 kHz). Synaptic currents were digitized off-line at 10 kHz (low-pass filtered at 2 kHz with an 8-pole Bessel filter) using pCLAMP9 software (Axon Instruments). The effects of drugs on the evoked EPSCs were assessed by averaging their amplitudes for 100 s (20 traces) after the effect had reached the steady state and comparing this value with the averaged amplitude of 20 traces just before the drug application. Statistical analysis was carried out using both Student's *t* test (two-tailed) and a non-parametric Mann–Whitney *U* test. A *P* value of 0.05 was used as the confidence limit and data are expressed as means ± S.E.M.

Drugs

Cy3-192IgG was custom-synthesized by Advanced Targeting Systems (San Diego, CA, USA). Synthetic ω-conotoxin GVIA (ω-CgTX), ω-agatoxin TK (ω-Aga-TK) and SNX-482 were purchased from Alamone Labs (Jerusalem, Israel). These toxins were dissolved in oxygenated perfusing solution containing cytochrome *c*

(1 mg ml^{-1}, Sigma). Other drugs were stored as frozen stock solutions and dissolved in the perfusing solution just before application in the final concentration indicated. 6-Cyano-7-nitroquinoxalline-2,3-dione (CNQX), D-(–)-2-amino-5-phosphonopentanoic acid (D-AP5) and bicuculline methochloride were from Tocris Cookson (Bristol, UK). (+/–)-6-chloro-7,8-dihydroxy-1-phenyl-2,3,4,5-tetrahydro-1H-3-benzazepine hydrobromide (SKF 81297), *R*(+)-7-chloro-8-hydroxy-3-methyl-1-phenyl-2,3,4,5-tetrahydro-1H-3-benzazepine hydrochloride (SCH 23390), dopamine, nifedipine, strychnine and forskolin were from Sigma (St Louis, MO, USA). All drugs were bath applied.

Immunofluorescence labelling for choline acetyltransferase (ChAT)

To confirm specific labelling of cholinergic neurones in the BF after Cy3-192IgG injection, choline acetyltransferase (ChAT) immunoreactivity in labelled cells was analysed. Four rats of similar age to those for the electrophysiological experiments were used. Five days following intracerebroventricular injection of Cy3-192IgG, rats were perfused with 4% paraformaldehyde in 0.1 M phosphate buffer containing 15% saturated picric acid solution. Their brains were removed and coronal brain slices (60 μm thick) were cut with a microslicer (DTK-1000, Dosaka). Three slices per animal (60 μm interval) containing HDB or SI were blocked with 10% normal goat serum (NGS) in Tris-HCl buffered saline (TBS, pH 7.4) containing 0.2% Triton X-100 for 1 h at room temperature, and reacted with a rabbit anti-ChAT primary antibody (1 : 2000 dilution in TBS containing 2% NGS and 0.2% Triton X-100; Chemicon) overnight at 4°C. Subsequently, sections were incubated in goat anti-rabbit IgG, conjugated with Alexa488 (1 : 500 dilution in the same solution for primary antibody; Molecular Probes) for 2 h at room temperature in the dark, and mounted on a slide glass with Vectashield (Vector Laboratory, CA, USA). One fluorescence image of the BF from each slice were acquired with a laser confocal microscope (FV300, Olympus Optics, Tokyo, Japan) with sequential acquisition of separate colour channels to avoid crosstalk between fluorochromes. Laser lights at 488 nm and 543 nm for excitation and emission lights at 510–530 nm and at > 570 nm were detected for Alexa488 and Cy3, respectively. Images were processed with Photoshop software (Adobe). When either the primary antibody or Cy3-192IgG injection was omitted, no fluorescence signal at a corresponding channel was obtained.

Results

Identification of BF cholinergic neurones

Whole-cell recordings were made from a total of 105 Cy3-192IgG-stained neurones within the HDB or SI of the BF region. Figure 1*A* shows BF neurones lying within a slice under infrared-differential interference contrast (IR-DIC) microscopy and Fig. 1*B* under fluorescence optics to reveal staining with Cy3-192IgG. In order to confirm that specific labelling in the BF after intracerebroventricular injections of Cy3-192IgG are cholinergic, colocalization of Cy3-192IgG signal and immunoreactivity for ChAT were verified. ChAT-immunopositive cells were frequently detected in both HDB and SI of the BF region, and its reactivity was distributed throughout the cytoplasm of dendrites, somata and axons of these cells (Fig. 1*C*). Cy3-192IgG-positive cells were also found in both subregions with lesser frequency than ChAT-positive cells, and the Cy3-192IgG signals showing a punctate appearance were localized mainly at the perikaya of cells (putative endosomes). All Cy3-192IgG-positive cells ($n = 124$ in 4 rats) were also positive for ChAT immunoreactivity, indicating that all Cy3-192IgG-labelled cells are cholinergic neurones.

Membrane properties and action potential firing were examined in the current-clamp mode and/or voltage-clamp mode with potassium gluconate-based internal solution in 15 out of these 105 neurones. In the voltage-clamp mode, application of hyperpolarizing step pulses from the holding potential of −65 mV produced non-linear changes in the currents. The current–voltage plots show inward rectification in all 10 neurones tested (Fig. 1*D*). In current-clamp mode, the resting membrane potential was -62.7 ± 0.54 mV ($n = 15$). In current-clamp, depolarizing current injection evoked action potentials. Hyperpolarizing current injections produced non-linear changes in the voltages, showing inward rectification. (Fig. 1*E*). The electrophysiological properties of these neurones are in good agreement with those previously reported on cholinergic neurones within the BF region (Griffith, 1988; Bengtson & Osborne, 2000; Wu *et al.* 2000). Therefore, Cy3-192IgG-positive cells were identified as cholinergic neurones and used in the following experiments on Ca^{2+}-channel subtypes involved in D_1-like receptor-mediated presynaptic inhibition.

Suppression of the evoked EPSCs by SKF 81297

All whole-cell recordings were made in the presence of bicuculline (10 μM), strychnine (0.5 μM) and D-AP5 (25 μM) to block $GABA_A$, glycine and NMDA glutamatergic components, respectively. Synaptic currents were evoked in Cy3-192IgG-stained cells by focal extracellular stimulation (50–120 μm radius of the recorded cell) at a rate of 0.2 Hz (every 5 s) from a holding potential of −65 mV. These synaptic currents were blocked by bath application of CNQX (5 μM) in all of the six cells tested (Fig. 2*A*), demonstrating that these synaptic currents are non-NMDA glutamatergic excitatory postsynaptic currents (EPSCs).

Bath application of SKF 81297 (SKF), a dopamine D_1-like receptor agonist, at a concentration of 30 μM, reversibly suppressed the amplitude of EPSCs as shown in Fig. 2*B*, consistent with our previous study (Momiyama *et al.* 1996). The suppressive effect reached steady state within a few minutes, and EPSCs recovered after 5–10 min washout (Fig. 2*B*). The inhibition of EPSC amplitude by initial application of SKF (30 μM) was $31.1 \pm 1.02\%$ ($n = 52$) of the control. In the following experiments, SKF was applied again after application of a dopamine D_1-like receptor antagonist or Ca^{2+} channel blocker and the effect of the second application of SKF was compared with that of the first. As shown in Fig. 2*B*, the SKF-induced inhibitory effect was reproduced upon second application. The inhibition of the second application of SKF was $28.8 \pm 1.93\%$ ($n = 6$), which was not significantly ($P > 0.05$, paired Student's t test) different from that of the first application in the respective neurones ($28.5 \pm 1.57\%$, $n = 6$, Fig. 2*C*).

Presynaptic origin of SKF-induced inhibition

To identify pre- or postsynaptic origin of SKF-induced inhibition of the EPSCs evoked in the identified cholinergic neurones, the effect of SKF on the paired-pulse facilitation (PPF) as well as the coefficient of variation (CV) were elucidated.

SKF-induced increase in PPF index of EPSCs. PPF has been regarded as an increase in transmitter release probability during the second stimulus in a paired-pulse protocol. The second response is facilitated compared with the first due to residual calcium transient in presynaptic terminals after the first stimulus (Neher, 1998; Zucker, 1999). PPF index was calculated from the following equation $[(EPSC_2 - EPSC_1)/EPSC_1]$, where $EPSC_1$ and $EPSC_2$ correspond to the peak amplitude of the first and second EPSCs, respectively, evoked in a paired-pulse protocol. Increases in PPF index would reflect changes in release probability, indicating that the effects originated from a presynaptic locus (Andreasen & Hablitz, 1994; Kamiya & Zucker, 1994; Kuhnt & Voronin, 1994). In the present experiments, SKF increased the PPF index in all of the nine neurones tested as shown in Fig. 3*A*. Mean PPF index before and after SKF application was 0.15 ± 0.03 and 0.54 ± 0.05 ($n = 9$, Fig. 3*B*), respectively. The difference in the PPF index between control and in the presence

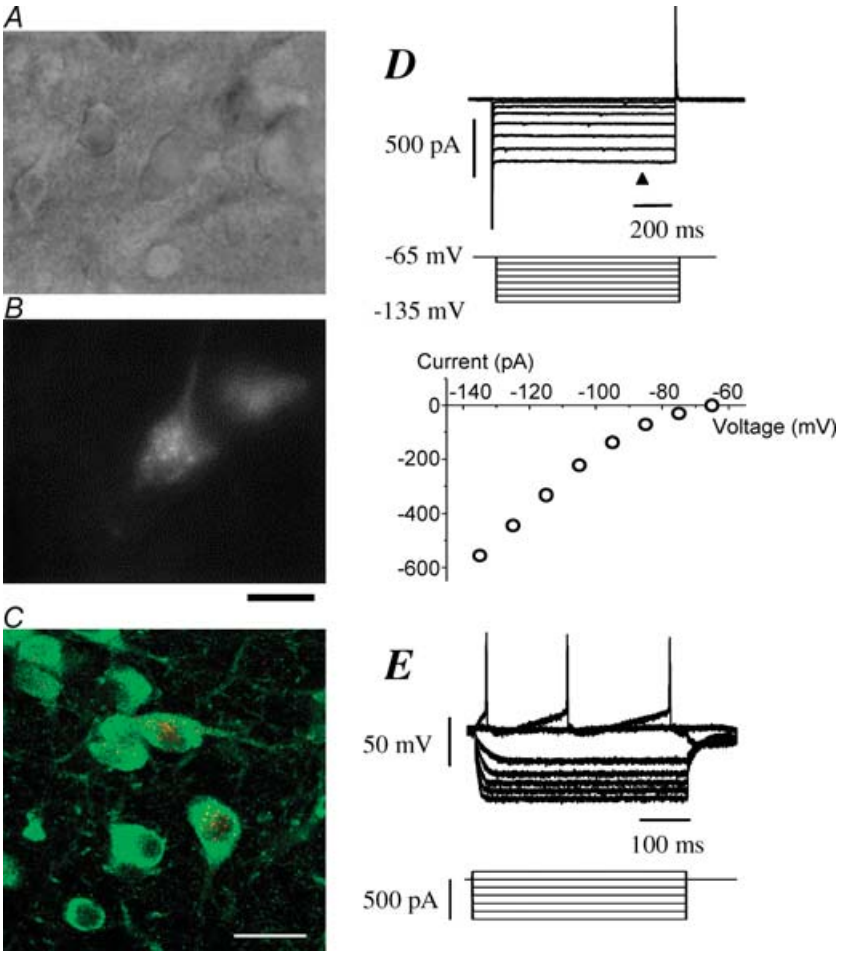

Figure 1. Morphological and electrophysiological identification of cholinergic neurones in the basal forebrain (BF)
A, BF neurones in a slice obtained from 15-day-old rat brain viewed under IR-DIC microscopy. The slice was 300 μm in thickness. *B,* the same neurones as in *A* in a fluorescent image labelled or unlabelled with Cy3-192IgG. Bar, 20 μm. *C,* Cy3-192IgG signals (red) in the BF and its colocalization with ChAT immunoreactivity (green) in the Cy3-192IgG-injected rats. Bar, 30 μm. *D,* membrane currents recorded from another BF neurone labelled with Cy3-192IgG in the voltage-clamp mode. The slice was obtained from 14-day-old rat brain. The neurone was held at −65 mV and hyperpolarizing voltage step pulses (middle traces) were applied through the recording pipette. Plots in the lower panel show the current–voltage relationship obtained from the upper current traces at the time point indicated by the arrowhead. Note the presence of inward rectification that is characteristic of cholinergic neurones in BF. *E,* membrane potentials and action potentials recorded in the current-clamp mode from the same neurone as in *D*, in response to the hyperpolarizing and depolarizing current pulses (lower traces). Note the non-linear changes in the voltages with the hyperpolarizing pulses, showing inward rectification. Cy3-192IgG (3 μl) was injected into the lateral ventricle of the ipsilateral side 4 days prior to the slice preparation. Whole-cell recordings were made with potassium gluconate-based internal solution.

of SKF was significant ($P < 0.05$, paired Student's t test, Fig. 3*B*). These results suggest that SKF-induced inhibition in cholinergic BF neurones is of presynaptic origin.

SKF-induced increase in CV of EPSCs. Coefficient of variation (CV) of synaptic currents is also another of the parameters used to determine the site of action, presynaptic or postsynaptic (Alger *et al.* 1996). CV is defined as: CV = s.D./mean = $[(1-p)/np]^{1/2}$, where p is release probability and n is the number of release site (Bekkers & Stevens, 1990); CV is dependent upon release probability and number of release sites, both presynaptic parameters, and is independent of quantal size, a post-synaptic parameter. Therefore, CV can be used to verify the presynaptic origin of SKF-induced effects (Manabe *et al.* 1993). In the present study, the CV value increased in all of the 52 cells during application of SKF. The mean CV value before SKF application was 0.25 ± 0.02 ($n = 52$), whereas the mean CV value in the presence of SKF increased to 0.36 ± 0.03 ($n = 52$, Fig. 3*C*). This increase is significant ($P < 0.05$, paired Student's t test), confirming a presynaptic origin for SKF-induced inhibition of the EPSCs.

The mean EPSC amplitude can be defined as qnp, where q is quantal size, if glutamate release is assumed to fit a binominal distribution. Therefore, we investigated whether SKF-induced inhibition may have resulted from a decrease in either q, n or p. Figure 3*D* shows the ratio, termed as $F = CV_{SKF}^{-2}/CV_{cont}^{-2}$ (where CV_{cont} is CV in control and CV_{SKF} is CV in the presence of SKF), is plotted against the ratio M ($EPSC_{SKF}/EPSC_{cont}$) where $EPSC_{SKF}$ is

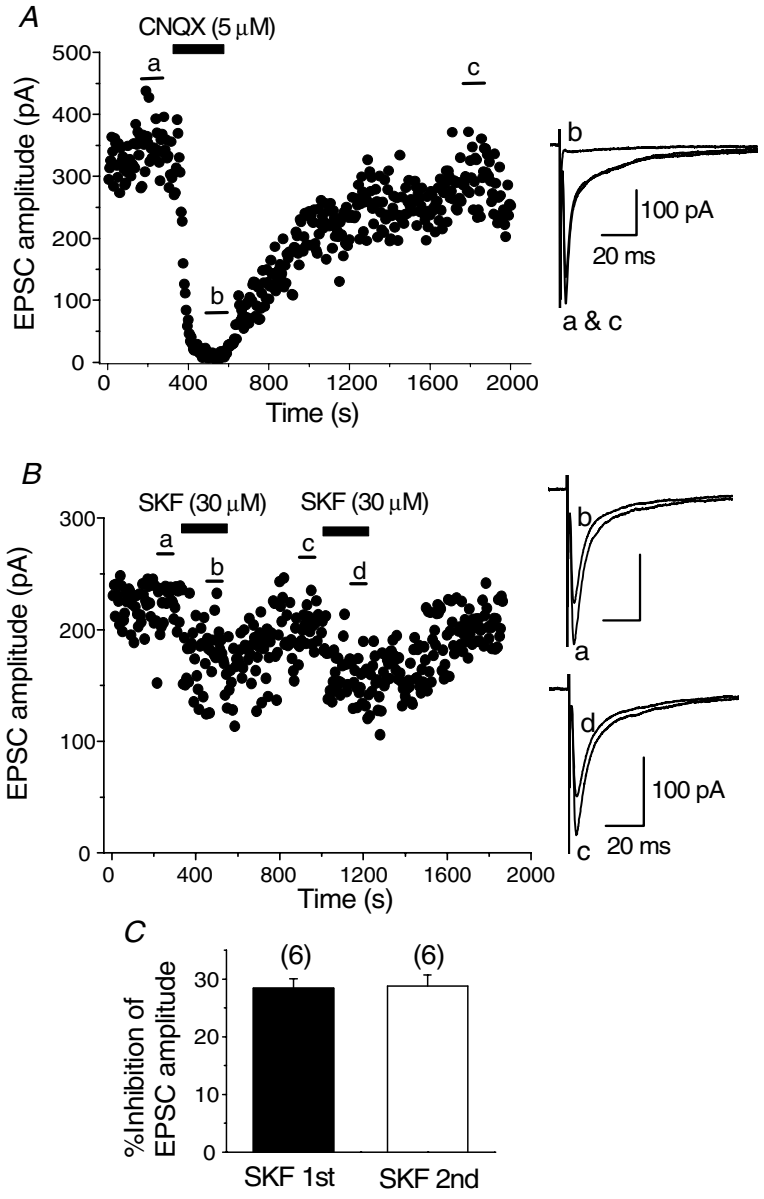

Figure 2. Inhibitory effect of SKF 81297 (SKF) on the evoked EPSCs
Synaptic currents were evoked at a rate of 0.2 Hz in the presence of bicuculline (10 μM), strychnine (0.5 μM) and D-AP5 (25 μM). The holding potential was −65 mV. *A,* time course of blockade of the evoked synaptic currents by CNQX (5 μM) and recovery on washout. CNQX was applied in the bath during the indicated period. Superimposed traces on the right show averages of 20 consecutive synaptic currents during the indicated periods in the time course plot. The synaptic currents were reversibly blocked by CNQX, suggesting that they are non-NMDA glutamatergic EPSCs. *B,* time course of the inhibition of the evoked EPSCs by SKF (30 μM) and recovery on washout. SKF was bath applied during the indicated periods. SKF was re-applied after the EPSCs had recovered from the inhibition induced by first application. In this and following figures (Figs 5, 6, 7 and 9), each point in the time course plot represents the amplitude of an individual synaptic current evoked at a rate of 0.2 Hz at the holding potential of −65 mV with CsCl-based internal solution. Superimposed traces on the right show averages of 20 consecutive EPSCs during the indicated periods in the time course plot. *C*, summarized histograms showing the inhibitory effect of SKF at first (SKF 1st) and second (SKF 2nd) application. The effect of second application was $28.8 \pm 1.93\%$ ($n = 6$), which was not significantly different ($P > 0.05$, paired Student's t test) from that of first application in the respective neurones ($28.5 \pm 1.57\%$, $n = 6$).

the mean EPSC during SKF application and $EPSC_{cont}$ is the mean EPSC in control. If SKF-induced inhibition of EPSCs resulted from a decrease in q, the value of F should be equal to 1, because F is independent of q. In this case, the plot data should fall on the line of $F = 1$. If SKF-induced EPSC inhibition resulted from a decrease in n, $F = M$, so the data points should fall on the line $F = M$. However, if SKF-induced inhibition resulted from a decrease in p, $F < M < 1$, then the data points should fall to the right of the line $F = M$ (Faber & Korn, 1991; Alger *et al.* 1996). As shown in Fig. 3*D*, 50 out of 52 of our data points did fall to the right of the line $F = M$, indicating a decrease in release probability, a presynaptic parameter. Thus, the findings using CV analysis, as those found with PPF, suggest a presynaptic locus for SKF-induced inhibition of the EPSCs in cholinergic BF neurones.

Antagonism by SCH 23390 on SKF-induced inhibition

To confirm that SKF-induced inhibition of EPSCs evoked in the identified cholinergic neurones were mediated by D_1-like dopamine receptors, we examined the effect of a D_1-like receptor antagonist, SCH 23390 (SCH, 10 μM), on the SKF (30 μM)-induced inhibition. In addition, the antagonistic effect of SCH was also investigated on dopamine (DA, 30 μM) itself. Application of SCH itself had no effect on the EPSCs in any of 11 neurones tested. After the EPSCs recovered from SKF- or DA-induced inhibition, SCH was applied in the bath for 10 min, before SKF was applied in the presence of SCH (Momiyama & Koga, 2001). As expected, the SKF-induced effect was antagonized by SCH (Fig. 4*Aa*), where SKF-induced inhibition in the presence of SCH was only 2.88 ± 0.67% ($n = 5$, Fig. 4*Ab*)

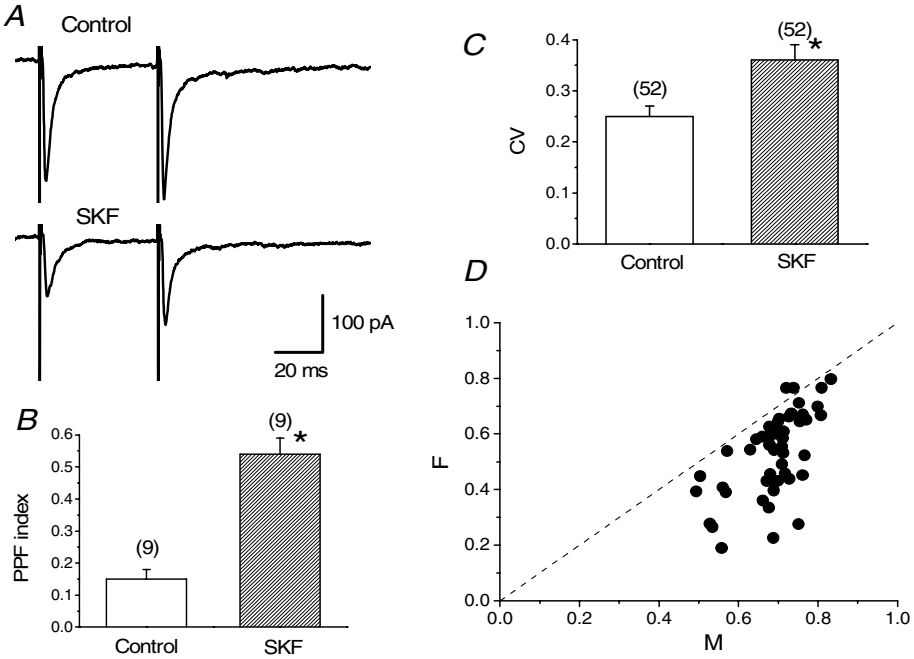

Figure 3. SKF-induced increase in paired-pulse facilitation (PPF) index and coefficient of variation (CV) of EPSCs

A, traces averaged from 20 consecutive EPSCs evoked with a paired-pulse protocol (interstimulus interval of 50 ms) at a rate of 0.2 Hz in control and during application of SKF (30 μM). PPF index was calculated from the equation of $(EPSC_2 - EPSC_1)/EPSC_1$. $EPSC_1$ and $EPSC_2$ correspond to the peak amplitude of first and second EPSCs, respectively, evoked with a paired-pulse protocol. *B,* summarized histograms showing the change in mean PPF index. SKF increased the PPF index in all of the 9 neurones examined. Mean PPF index during SKF application (0.54 ± 0.05, $n = 9$) was significantly larger (*$P < 0.05$, paired Student's t test) than that before SKF application (0.15 ± 0.03, $n = 9$). *C,* summarized histograms showing the change in mean CV before and after application of SKF. SKF increased CV value in all of the 52 neurones tested. Mean CV value during application of SKF (0.36 ± 0.03, $n = 52$) was significantly larger (*$P < 0.05$, paired Student's t test) than that in control (0.25 ± 0.02, $n = 52$). *D,* the square of coefficient of variation (CV^2) of evoked EPSC amplitude was compared before and during application of SKF, and the ratio of CV^2 before ($CV_{cont}{}^2$) and during SKF application ($CV_{SKF}{}^2$) ($CV_{SKF}{}^{-2}/CV_{cont}{}^{-2}$, termed F) was plotted against the ratio of the mean amplitude of EPSCs during SKF application ($EPSC_{SKF}$) compared with that in control period ($EPSC_{cont}$) ($EPSC_{SKF}/EPSC_{cont}$, termed M). Results are from 52 cells, in all of which the CV value increased during SKF application. The line $F = M$ and to the right of it correspond to the location of data points in which the change is presynaptic.

as compared with $27.6 \pm 2.35\%$ ($n = 5$, Fig. 4*Ab*), an inhibition obtained in the absence of SCH. Similarly, DA-induced inhibition of the EPSCs was antagonized by SCH (Fig. 4*Ba*). DA-induced inhibition in the presence of SCH was $4.24 \pm 1.40\%$ ($n = 6$, Fig. 4*Bb*) whilst by DA alone produced an inhibition of $30.0 \pm 6.12\%$ ($n = 6$, Fig. 4*Bb*).

Calcium channel subtypes contributing to the EPSCs

Previous studies in several central synapses have shown that multiple Ca^{2+} channel subtypes are involved in excitatory or inhibitory transmission (Takahashi & Momiyama, 1993; Wheeler *et al.* 1994; Iwasaki *et al.* 2000; Momiyama & Koga, 2001). In the present study, we examined the contribution of calcium channel subtypes underlying the EPSCs in identified cholinergic BF neurones. Bath application of an N-type Ca^{2+} channel blocker, ω-CgTX at a saturating concentration (3 μM; Takahashi & Momiyama, 1993), gradually decreased the amplitude of the EPSCs and the effect reached the steady state in 5–10 min, as shown in Fig. 5*A*. The remaining fraction of the EPSCs after the ω-CgTX-induced effect had reached the steady state was largely blocked by the subsequent application of a P/Q-type Ca^{2+} channel blocker, ω-Aga-TK (200 nM; Takahashi & Momiyama, 1993). Figure 5*B* shows the time course of inhibition of the EPSCs when ω-Aga-TK (200 nM) was applied first. The remaining fraction of the EPSCs after the ω-Aga-TK-induced effect had reached the steady state was largely blocked by the subsequent application of ω-CgTX (3 μM). Pooled data show that inhibition of EPSCs by ω-CgTX (3 μM), ω-Aga-TK (200 nM) and both toxins were $57.5 \pm 2.27\%$ ($n = 16$), $68.9 \pm 1.71\%$ ($n = 20$), and $96.1 \pm 0.27\%$ ($n = 10$), respectively (Fig. 5*C*). In order to further identify the profile of Ca^{2+} channels resistant to both ω-CgTX and ω-Aga-TK, that is non-N-, non-P/Q-type, contributing to the excitatory transmission onto BF cholinergic neurones, the effects of two additional Ca^{2+} channel blockers were tested: SNX-482, an R-type channel blocker at a saturating concentration (300 nM; Newcomb *et al.* 1998; Wang *et al.* 1999; Daniel *et al.* 2004), and nifedipine, a well-known L-type channel blocker (10 μM; for review see Triggle, 2006). The inhibitory effect of SNX-482 (300 nM) on the EPSC amplitude was not so prominent, compared with that of ω-CgTX or ω-Aga-TK. Pooled data show that the inhibition by SNX-482 (300 nM) was $18.3 \pm 5.70\%$ ($n = 7$) of the control (Fig. 5*C*). Similarly to the case of other central synapses (Takahashi & Momiyama, 1993), nifedipine had little effect. Pooled

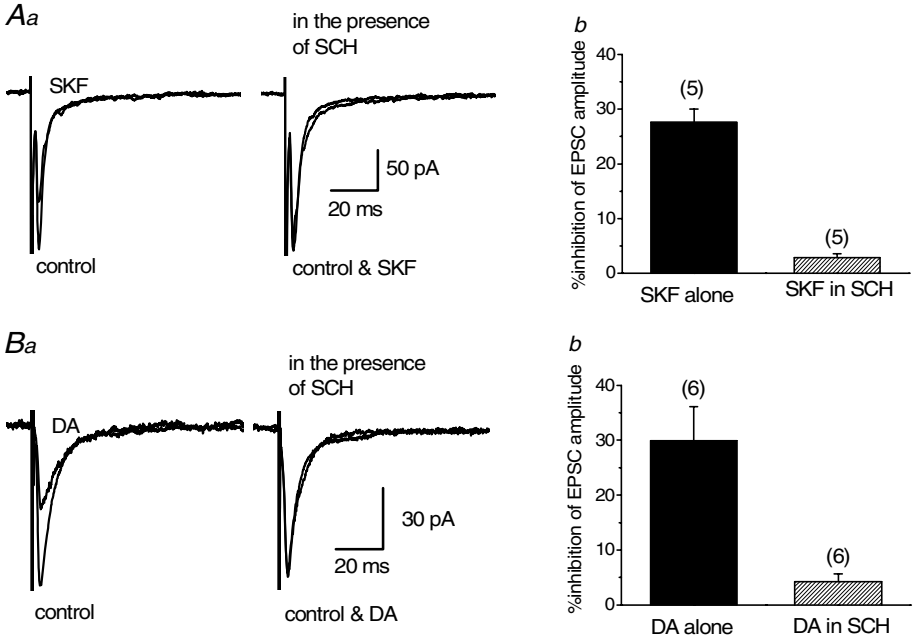

Figure 4. Antagonizing effect of SCH 23390 (SCH) on SKF- or dopamine (DA)-induced inhibition of EPSCs
Effect of SKF (30 μM, *A*) or DA (30 μM, *B*) on the EPSCs in the presence of SCH (10 μM) was compared with that of SKF or DA alone. Each trace in *Aa* and *Ba* is the superimposed averages of 20 consecutive EPSCs before (control) and during application of SKF or DA. SCH was applied for 10 min before second application of SKF or DA. *Ab* and *Bb,* histograms summarizing the mean inhibitory effects of SKF (*Ab*) and DA (*Bb*) in the absence and presence of SCH. Error bars indicate S.E.M. *Ab,* value in the presence of SCH ($2.88 \pm 0.67\%$, $n = 5$) was significantly smaller ($P < 0.05$, paired Student's *t* test) than that of SKF alone in the corresponding neurones ($27.6 \pm 2.35\%$, $n = 5$). *Bb,* value in the presence of SCH ($4.24 \pm 1.40\%$, $n = 6$) was significantly smaller ($P < 0.05$, paired Student's *t* test) than that of DA alone in the corresponding neurones ($30.0 \pm 6.12\%$, $n = 6$).

data show that the nifedipine (10 μM)-induced inhibitory effect was 4.70 ± 1.80% ($n = 5$) of the control (Fig. 5*C*).

Ca^{2+} channel subtypes involved in the inhibitory action of SKF

After recovery of the EPSCs from the inhibition induced by initial application of SKF (30 μM), one of the Ca^{2+} channel blockers was applied, and after the effect had reached a steady state, SKF was re-applied. As shown in Fig. 6*A*, SKF could still induce an inhibition on the amplitude of EPSCs in the presence of ω-CgTX (3 μM), the inhibitory effect by SKF being 31.5 ± 5.86% ($n = 4$) of control in ω-CgTX, which was not significantly different ($P > 0.05$, paired Student's t test) from that induced in its absence in the respective neurones (30.9 ± 3.18%, $n = 4$, Fig. 6*A*, and also see pooled data shown in Fig. 8). On the other hand, after ω-Aga-TK (200 nM), SKF no longer affected the EPSCs (Fig. 6*B*). The inhibitory effect induced by SKF in the presence of ω-Aga-TK was 4.97 ± 1.34% ($n = 7$), which was significantly smaller ($P < 0.05$, paired Student's t test) than that obtained by SKF before ω-Aga-TK application in the respective neurones (37.9 ± 3.83%, $n = 7$, Fig. 6*B*, and pooled data in Fig. 8). The effect of SKF on EPSCs was not affected by either SNX-482 (300 nM) or nifedipine (10 μM). The degree of the inhibitory effect of SKF on EPSCs was not significantly different ($P > 0.05$, paired Student's t test) before and after the application of SNX-482 (31.8 ± 3.26% and 30.2 ± 3.61%, respectively, in 7 neurones, Fig. 8). Similarly, there was

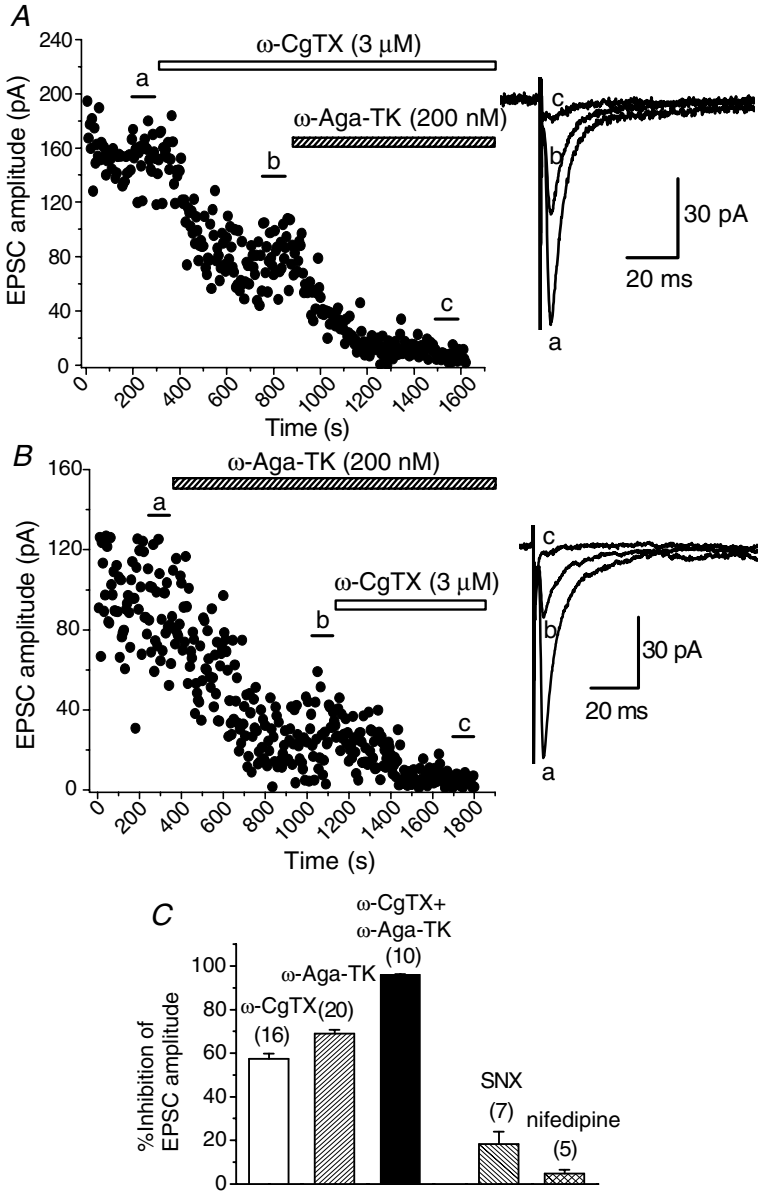

Figure 5. Suppression of the EPSCs by ω-CgTX and ω-Aga-TK
A and *B*, time course of the inhibitory effects of ω-CgTX (3 μM, *A*) and ω-Aga-TK (200 nM, *B*) on the amplitude of EPSCs. Toxins were bath applied during the indicated periods. *A*, ω-CgTX reduced the amplitude of EPSCs by 49.0% of control. *B*, ω-Aga-TK reduced the amplitude of EPSCs by 66.3% of control. Subsequent application of ω-Aga-TK (*A*) or ω-CgTX (*B*) almost blocked the remaining EPSCs. Superimposed sample records at the right of *A* and *B* are the averages of 20 consecutive EPSCs during the indicated periods. *C*, histograms summarizing the suppression of the EPSCs by ω-CgTX (3 μM), ω-Aga-TK (200 nM), SNX-482 (SNX, 300 nM) and nifedipine (10 μM). Values for ω-CgTX, ω-Aga-TK, both ω-CgTX and ω-Aga-TK, SNX and nifedipine are 57.5 ± 2.27% ($n = 16$), 68.9 ± 1.71% ($n = 20$), 96.1 ± 0.27% ($n = 10$), 18.3 ± 5.70 ($n = 7$) and 4.70 ± 1.80 ($n = 5$), respectively.

no significant difference ($P > 0.05$, paired Student's t test) in SKF-induced inhibition before and after application of nifedipine (31.6 ± 0.35% and 30.6 ± 2.36%, respectively, in 4 neurones, Fig. 8).

The possibility could not be excluded that the small effect of SKF after application of ω-Aga-TK was the result of high co-operativity of P/Q channels to transmitter release (Reid *et al.* 1998). To examine this issue, the following experiments were carried out. After the EPSCs recovered from SKF-induced inhibition, ω-CgTX or ω-Aga-TK was applied. After the effects of the toxins had reached the steady state, the concentration of Ca^{2+} in the perfusing solution was increased to 7.2 mM (3 times as high as the control solution) so as to enhance the EPSC amplitude, and then SKF was re-applied. As shown in Fig. 7*A*, increasing Ca^{2+} concentration recovered the EPSC amplitude nearly to the level before application of ω-CgTX. Pooled data show that increasing the concentration of Ca^{2+} enhanced the EPSC amplitude to 175.5 ± 10.7% ($n = 6$) compared with the value in the steady state of the ω-CgTX-induced effect. Under this condition, SKF still inhibited the EPSCs by similar degrees to that observed in the initial SKF application (Fig. 7*A*). SKF-induced inhibition in 7.2 mM Ca^{2+} after application of ω-CgTX was 33.2 ± 4.41% ($n = 6$, Fig. 8), a value that was not significantly different ($P > 0.05$, paired Student's t test) from that induced by the initial SKF application (27.9 ± 2.27%, $n = 6$, Fig. 8). On the other hand, the recovery of EPSC amplitude by increasing Ca^{2+} concentration was not so prominent after ω-Aga-TK-induced effect had reached its steady state (Fig. 7*B*). Pooled data show that EPSC amplitude in 7.2 mM Ca^{2+} was 139.0 ± 13.3% ($n = 7$) of the value of the standard Ca^{2+} concentration in the presence of ω-Aga-TK. Such a difference between ω-CgTX and ω-Aga-TK has been observed in a previous study (Reid *et al.* 1998). Even in this high Ca^{2+} condition, SKF had no further inhibitory effect in the presence of ω-Aga-TK. SKF-induced inhibition in 7.2 mM Ca^{2+} after application of ω-Aga-TK was 3.37 ± 0.55% ($n = 7$, Fig. 8), significantly smaller ($P < 0.05$, paired Student's t test) than that induced by the initial SKF application (30.9 ± 3.66%, $n = 7$, Fig. 8).

Effect of Ca^{2+} channel blockers on forskolin-induced inhibition of EPSCs

D_1-like DA receptors have been classified as those positively coupled with adenylyl cyclase activity (Kebabian & Calne,

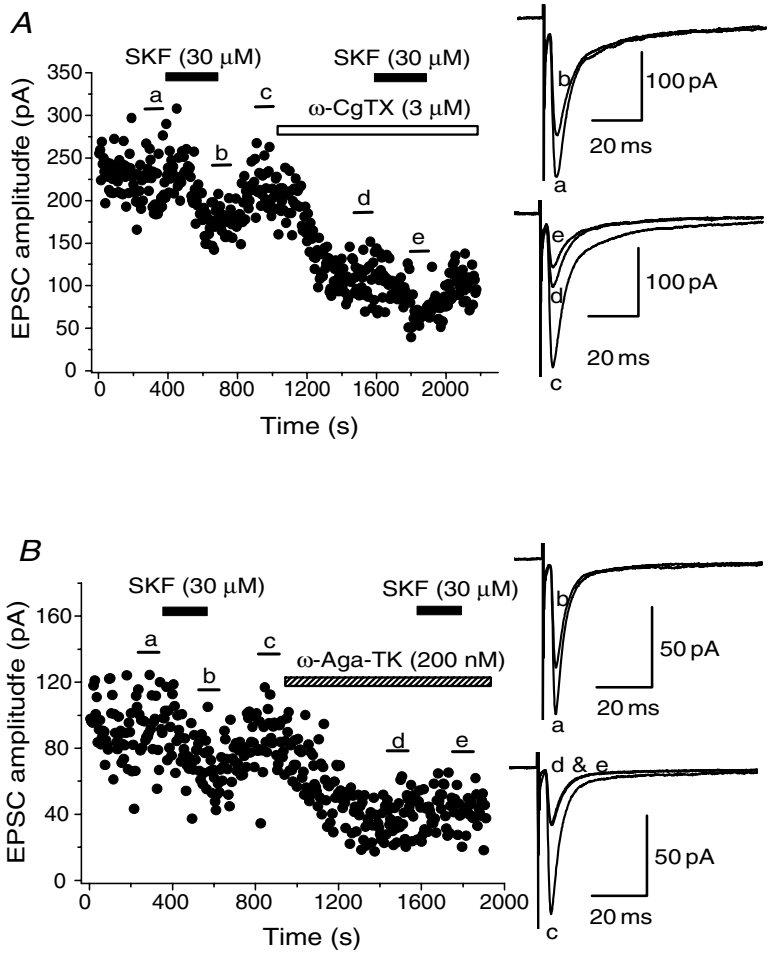

Figure 6. Occlusion of SKF –induced inhibition by ω-Aga-TK, and not by ω-CgTX
Time course of the effect of SKF (30 μM) on EPSCs before and after application of ω-CgTX (3 μM, *A*) or ω-Aga-TK (200 nM, *B*). SKF, ω-CgTX and ω-Aga-TK were applied in the bath during the indicated periods. Toxins were applied after EPSCs had recovered from the inhibition induced by the initial application of SKF. After the suppression by ω-CgTX or ω-Aga-TK had reached steady state, SKF was applied again. Superimposed sample records at the right of both panels are the averages of 20 consecutive EPSCs during the indicated periods.

1979). We have previously reported that D_1-like receptors share common mechanisms with the adenylyl cyclase pathway for presynaptic inhibition of glutamate release onto magnocellular BF neurones (Momiyama *et al.* 1996). Therefore, we examined whether blockade of P/Q-type Ca^{2+} channels, that have been suggested to be effector proteins downstream of D_1-like receptors, could affect the inhibitory effect of forskolin (FK), an activator of the adenylyl cyclase pathway. Similar to the case of our previous study, bath application of FK (10 μM) reduced the amplitude of the EPSCs within 10–15 min of application (Fig. 9*A*). The inhibition by FK (10 μM) was 35.3 ± 1.31% ($n = 4$, Fig. 9*D*). After the effect of ω-CgTX (3 μM) had reached steady state, FK still inhibited the EPSCs (Fig. 9*B*). The inhibitory effect by FK in the presence of ω-CgTX (3 μM) was 35.2 ± 2.74% ($n = 5$, Fig. 9*D*), a value that is not significantly different ($P > 0.05$) from the value of FK alone. On the other hand, after the effect of ω-Aga-TK (200 nM) had reached its steady state, FK-induced inhibitory effect was reduced (Fig. 9*C*). FK-induced inhibition after application of ω-Aga-TK (200 nM) was 9.31 ± 2.92% ($n = 5$, Fig. 9*D*), significantly smaller ($P < 0.05$) than that of FK alone.

Discussion

The present results suggest that activation of presynaptic D_1-like receptors selectively blocks P/Q-type Ca^{2+} channels to reduce glutamate release onto identified BF cholinergic neurones. We have previously reported

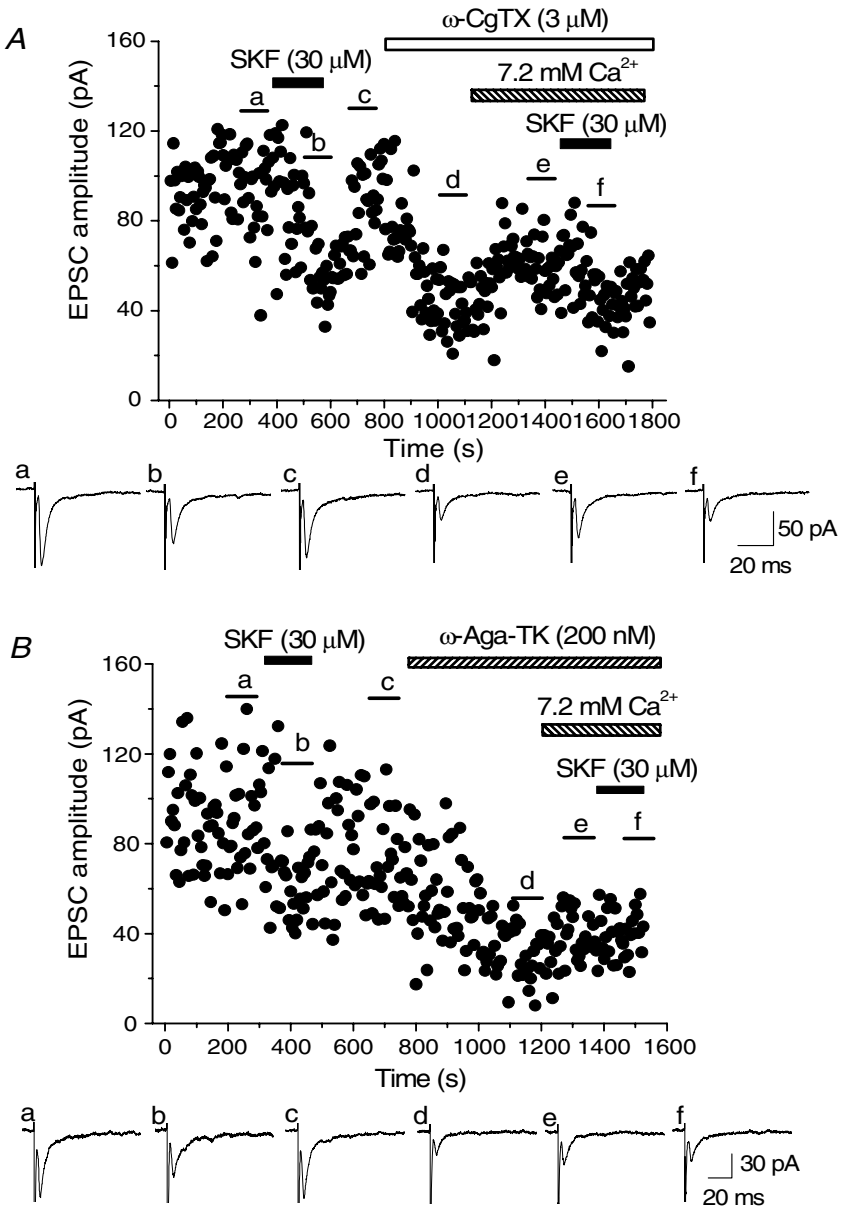

Figure 7. Effects of ω-CgTX- or ω-Aga-TK on the SKF-induced inhibition in high extracellular Ca^{2+}
Time course of inhibition by SKF (30 μM) on EPSCs before and after application of ω-CgTX (3 μM, *A*) or ω-Aga-TK (200 nM, *B*) and increasing extracellular Ca^{2+} ($[Ca^{2+}]$) to 7.2 mM. SKF, ω-CgTX and ω-Aga-TK were applied in the bath during the indicated periods. Toxins were applied following full recovery of EPSCs from the initial application of SKF. After the suppression by ω-CgTX or ω-Aga-TK had reached steady state, $[Ca^{2+}]$ was increased to 7.2 mM during the indicated periods, and then SKF was re-applied. Sample records shown below the time course plot in both panels are the averages of 20 consecutive EPSCs during the indicated periods.

that activation of D_1-like receptors presynaptically inhibits glutamate release onto magnocellular neurones in the BF region. However, morphologically identified magnocellular neurones include not only cholinergic but also GABAergic and glutamatergic neurones (Saper, 1984; Gritti *et al.* 1997; Manns *et al.* 2001). In the present study, BF cholinergic neurones were identified as Cy3-192IgG-positive cells. The electrophysiological properties of neurones stained with Cy3-192IgG agreed well with those of immunohistochemically identified cholinergic neurones in the BF region (Griffith, 1988; Bengtson & Osborne, 2000). Furthermore, in the present study, immunohistochemical confirmation was carried out with ChAT staining in Cy3-192IgG-positive neurones. Therefore, the present results confirmed that Cy3-192IgG is a useful marker for BF cholinergic neurones. Since the present study is the first report on the effect of D_1-like receptor activation on the synaptic transmission onto Cy3-192IgG-labelled BF neurones, we investigated and confirmed the dopamine receptor pharmacology and presynaptic locus of action.

In the previous study (Momiyama *et al*. 1996) we have also shown that D_1-like receptor-mediated presynaptic inhibition of EPSCs is dependent of external Ca^{2+}, suggesting that activation of D_1-like receptors block Ca^{2+} entry into presynaptic terminals. Presynaptic regulation of Ca^{2+} entry could be mediated by either direct effect on Ca^{2+} channels or indirect effect through potassium channels. In the present study, we initially undertook to clarify the Ca^{2+} channel subtypes involved in the non-NMDA glutamatergic transmission onto BF cholinergic neurones. Similarly to the cases of other central synapses, the excitatory transmission was found to be regulated by multiple types of Ca^{2+} channels (Luebke *et al.* 1993; Takahashi & Momiyama, 1993; Regehr & Mintz, 1994; Umemiya & Burger, 1994; Wheeler *et al.* 1994; Wu & Saggau, 1994; Wu *et al.* 1998; Iwasaki *et al.* 2000; Momiyama & Koga, 2001). The overlap in the effect of ω-CgTX and ω-Aga-TK (Fig. 5*C*) might be explained by a non-linear relationship between presynaptic calcium concentration and transmitter release in several central synapses (Jenkinson, 1957; Dodge & Rahamimoff, 1967; Augustine & Charlton, 1986; Takahashi & Momiyama, 1993; Momiyama & Koga, 2001). Assuming such a non-linear relationship between presynaptic Ca^{2+} concentration and transmitter release, a considerable portion of the transmission could be regulated by channels resistant to both ω-CgTX and ω-Aga-TK, that is, non-N-, non-P/Q-type channels (Takahashi & Momiyama, 1993; Momiyama & Koga, 2001). In the present study, SNX-482, an R-type Ca^{2+} channel blocker, did not show prominent effect on the EPSCs, and nifedipine, an L-type Ca^{2+} channel blocker, had little effect. In addition, previous studies indicate that usual dihydropyridine antagonists are ineffective on L-type voltage-dependent Ca^{2+} channels in the CNS presynaptic terminals (Bell *et al.* 2001; Xu & Lipscombe, 2001). Therefore, SNX-482-resistant R-type channels and/or other unidentified types of Ca^{2+} channels could be involved in the glutamatergic transmission onto BF cholinergic neurones. Although the Ca^{2+} channel subtypes contributing to the glutamatergic transmission have not been completely identified in the present study, SKF had no effect on EPSCs after the effect of ω-Aga-TK had reached steady state whilst it could still inhibit EPSCs after ω-CgTX application, suggesting that activation of D_1-like receptors directly and selectively block P/Q-type Ca^{2+} channels to reduce glutamate release.

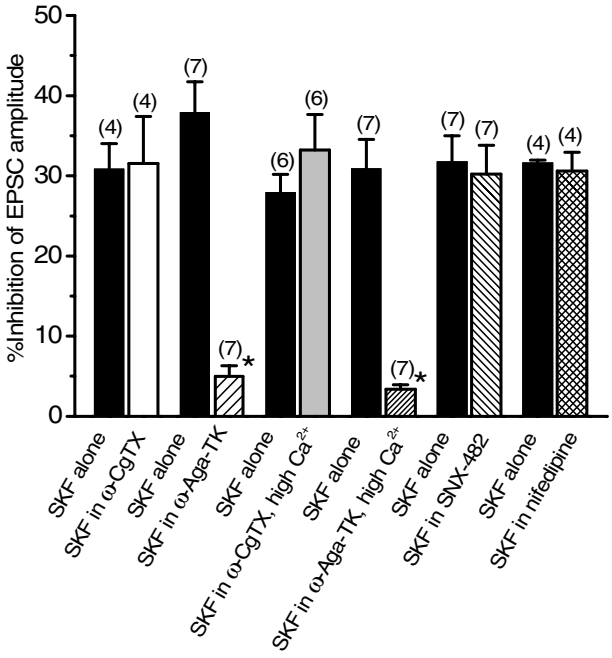

Figure 8. Summarized histograms showing the effects of Ca^{2+} channel blockers on the SKF (30 μM)-induced inhibition of the EPSCs

SKF-induced inhibition in the presence of each Ca^{2+} channel blocker was compared with that induced by SKF alone in the respective neurone group. Once the effect of ω-Aga-TK had reached steady state, SKF-induced inhibition of the EPSC amplitude was only $4.97 \pm 1.34\%$ ($n = 7$), significantly smaller ($^*P < 0.05$) than that induced by SKF alone ($37.9 \pm 3.83\%$, $n = 7$), whereas SKF still inhibited the EPSCs after the other Ca^{2+} channel blockers had reached steady state. SKF-induced inhibition of the EPSC amplitude in the presence of ω-CgTX, SNX-483 or nifedipine was $31.5 \pm 5.86\%$ ($n = 4$), $30.2 \pm 3.61\%$ ($n = 7$) or $30.6 \pm 2.36\%$ ($n = 4$), respectively. Each of these values was not significantly different ($P > 0.05$) from the corresponding value by SKF alone ($30.9 \pm 3.18\%$ ($n = 4$), $31.8 \pm 3.26\%$ ($n = 7$) or $31.6 \pm 0.35\%$ ($n = 4$), respectively). SKF-induced inhibition in 7.2 mM Ca^{2+} solution after application of ω-Aga-TK ($3.37 \pm 0.55\%$, $n = 7$) was significantly smaller ($^*P < 0.05$) than that induced by initial SKF application ($30.9 \pm 3.66\%$, $n = 7$), whereas SKF-induced inhibition in high Ca^{2+} after ω-CgTX application (33.2 ± 4.41, $n = 6$) was not significantly different ($P > 0.05$) from that by SKF alone ($27.9 \pm 2.27\%$, $n = 6$). Statistical significance in each group was determined by paired Student's *t* test.

Although transmitter release and Ca^{2+} entry are non-linearly related as mentioned above, the cooperativity is dependent on Ca^{2+} channel subtypes, particularly on their association with exocytotic machinery, the power coefficient being between 1 and 4 (or even more) (Wu & Saggau, 1994; Mintz *et al.* 1995; Borst & Sakmann, 1996; Takahashi *et al.* 1996; Reid *et al.* 1998; Wu *et al.* 1998). This issue would be clarified if the relationship between external Ca^{2+} concentration and EPSC amplitude was investigated under pharmacological blockade of each Ca^{2+} channel subtype. However, this would be out of the scope of the present study. Regarding this issue, the possibility might not be excluded that little effect of SKF after application of ω-Aga-TK was due to high Ca^{2+} cooperativity of P/Q type channels for transmitter release. However, this possibility was not likely in the present study, since SKF had no further effect on the EPSCs even when external Ca^{2+} concentration was increased after application of ω-Aga-TK. These findings suggest, for the first time, a specific coupling between presynaptic D_1-like receptors and P/Q-type Ca^{2+} channels.

D_1-like dopamine receptors have been categorized as those positively coupled with adenylyl cyclase activity (Kebabian & Calne, 1979). It has been shown that forskolin (FK), which stimulates adenylyl cyclase activity and increases intracellular cyclic AMP levels, suppresses the EPSC amplitude evoked in magnocellular BF neurones, and occludes D_1-like receptor-mediated presynaptic inhibition of the EPSCs (Momiyama *et al.* 1996). In the present study, FK-induced suppression of EPSCs was confirmed in morphologically identified cholinergic BF neurones. Furthermore, the present study

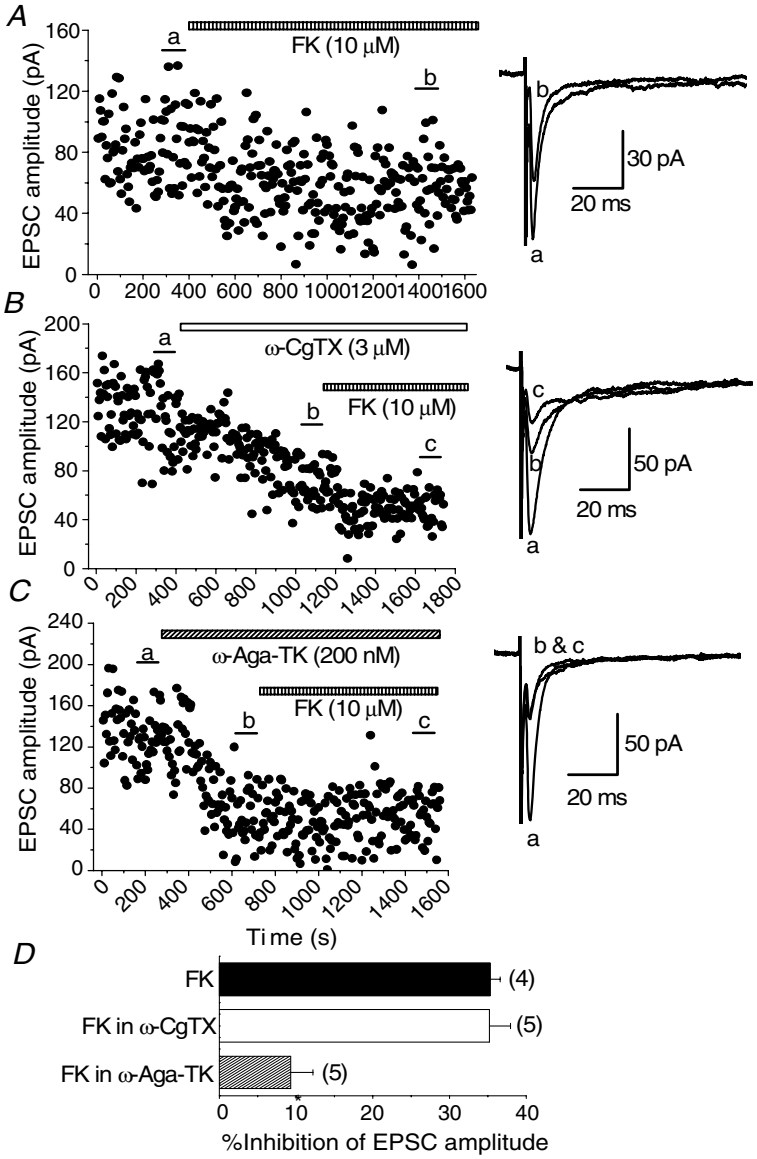

Figure 9. Effect of ω-CgTX and ω-Aga-TK on forskolin (FK)-induced inhibition of EPSCs
A, time course of the inhibitory effect of FK (10 μM) on the EPSCs. *B,* FK could still inhibit the EPSCs in the presence of ω-CgTX (3 μM). *C,* FK had no effect in the presence of ω-Aga-TK (200 nM). Superimposed sample records at the right of *A, B* and *C* are the averages of 20 consecutive EPSCs during the indicated periods. *D,* summarized histograms showing the effect of ω-CgTX and ω-Aga-TK on FK-induced inhibition of EPSCs. The inhibition by FK alone was 35.3 ± 1.31% ($n = 4$). FK-induced inhibition in the presence of ω-Aga-TK (9.31 ± 2.92%, $n = 7$) was significantly smaller (*$P < 0.05$) than that by FK alone, whereas FK-induced inhibition in ω-CgTX (35.2 ± 2.74%, $n = 5$) was not significantly different ($P < 0.05$) from that of FK alone.

has demonstrated that the inhibitory effect of FK is mostly blocked by pre-application of ω-Aga-TK, but not by ω-CgTX, suggesting a link between the adenylyl cyclase system and P/Q-type Ca^{2+} channels. The remaining effect of FK even after application of ω-Aga-TK (Fig. 9*D*) indicates that the other effectors mediated by adenylyl cyclase system are involved in the synaptic transmission. The intracellular signalling mechanisms linking the adenylyl cyclase system and P/Q-type channels are unknown. It has been shown in striatal medium spiny neurones that activation of D_1-like receptors enhances the activity of a protein phosphatase (PP1) via cyclic AMP-dependent protein kinase, thereby reducing N- or P/Q-type Ca^{2+} currents (Surmeier *et al.* 1995). It remains to be elucidated whether this pathway is available to the present glutamatergic synapses onto BF cholinergic neurones. In addition, dopamine receptor-interacting proteins (DRIPs) have been functionally characterized (Lezcano *et al.* 2000; Bergson *et al.* 2003). The crosstalk between the adenylyl cyclase pathway and DRIPS modulating presynaptic Ca^{2+} channels also remains unknown. Several studies have investigated coupling between Ca^{2+} channel subtypes and presynaptic G-protein-coupled receptors in central synapses, such as metabotropic glutamate receptors (Takahashi *et al.* 1996; Stefani *et al.* 1998), or adenosine receptors (Umemiya & Berger, 1994; Kimura *et al.* 2003). These receptors include those in which there is no selective coupling with a certain type of Ca^{2+} channel subtype. The unique profiles of dopamine receptors have been shown by the selective coupling between D_1-like receptors and P/Q-type channels clarified in the present study, as well as previously reported specific coupling between presynaptic D_2-like receptors and N-type Ca^{2+} channels in GABAergic transmission onto striatal cholinergic interneurones (Momiyama & Koga, 2001). Such characteristics might be attributed to intracellular messenger systems mentioned above.

In several mammalian central synapses, the contribution of N-type channels declines with development (Iwasaki *et al.* 2000; Momiyama, 2003). In addition, D_2-like dopamine receptor-mediated presynaptic inhibition decreases with age in parallel with the decline in the contribution of the N-type channel (Momiyama, 2003). It remains to be elucidated whether the present coupling between presynaptic D_1-like receptors and P/Q-type Ca^{2+} channels undergoes such a developmental change.

P/Q-type Ca^{2+} channels are widely distributed in the central nervous system and mediate a considerable part of fast synaptic transmission at a variety of central synapses (Takahashi & Momiyama, 1993; Wheeler *et al.* 1994). In addition, a mutation in P/Q-type Ca^{2+} channels has been shown to lead to the appearance of absence epilepsy (Mori *et al.* 1991; Fletcher *et al.* 1996), a possible underlying mechanism being impaired feedforward inhibition in the thalamocortical synapses (Sasaki *et al.* 2006). On the other hand, it has been suggested that the BF cholinergic system is implicated in attention, motivation or memory (Arendt *et al.* 1989; Dunnett & Fibiger, 1993; Muir *et al.* 1994) as well as in a number of neuropsychiatric disorders such as Alzheimer's disease and schizophrenia (Price *et al.* 1986; Mann, 1988; Perry *et al.* 1993; Gaula & Mesulam, 1994). Therefore, the present findings suggest another function of Ca^{2+} channel subtypes in these neuropsychiatric functions. The present results also indicate that Ca^{2+} channel-related drugs could be at least one of the therapeutic tools for BF-related disorders.

References

Alger BE, Pitler JJ, Wagner JJ, Martin LA, Morishita W, Kirov SA & Lenz RA (1996). Retrograde signalling in depolarization-induced suppression of inhibition in rat hippocampal CA1 cells. *J Physiol* **496**, 197–209.

Andreasen M & Hablitz JJ (1994). Paired-pulse facilitation in the dentate gyrus: a patch-clamp study in rat hippocampus in vitro. *J Neurophysiol* **72**, 326–336.

Arendt T, Allen Y, Marchbanks RM, Schugens MM, Sinden J, Lantos PL & Gray GA (1989). Cholinergic system and memory in the rat: effects of chronic ethanol, embryonic basal forebrain brain transplants and excitotoxin lesions of cholinergic basal forebrain projection system. *Neuroscience* **33**, 435–462.

Augustine GJ & Charlton MP (1986). Calcium dependence of presynaptic calcium current and post-synaptic response at the squid giant synapse. *J Physiol* **381**, 619–640.

Batchelor PE, Armstrong DM, Blaker SN & Gage FH (1989). Nerve growth factor receptor and choline acetyltransferase colocalization in neurons within the rat forebrain: response to fimbria-fornix transection. *J Comp Neurol* **284**, 187–204.

Bekkers JM & Stevens CF (1990). Presynaptic mechanism for long-term potentiation in the hippocampus. *Nature* **346**, 724–729.

Bell DC, Butcher AJ, Berrow NS, Page KM, Brust PF, Nesterova A, Stauderman KA, Seabrook GR, Nrmberg B & Dolphin AC (2001). Biophysical properties, pharmacology, and modulation of human, neonatal L-type ($\alpha_{;1D}$, $Ca_V1.3$) voltage-dependent calcium currents. *J Neurophysiol* **85**, 816–827.

Bengtson CP & Osborne PB (2000). Electrophysiological properties of cholinergic and noncholinergic neurons in the ventral pallidal region of the nucleus basalis in rat brain slice. *J Neurophysiol* **83**, 2649–2660.

Bergson C, Levenson R, Goldman-Rakic PS & Lidow MS (2003). Dopamine receptor-interacting proteins: the Ca^{2+} connection in dopamine signaling. *Trends Pharmacol Sci* **24**, 486–492.

Borst JG & Sakmann B (1996). Calcium influx and transmitter release in a fast CNS synapse. *Nature* **383**, 431–434.

Coyle JT, Price DL & DeLong MR (1983). Alzheimer's disease: a disorder of cortical cholinergic innervation. *Science* **219**, 1184–1190.

Daniel H, Rancillac A & Crepel F (2004). Mechanisms underlying cannabinoid inhibition of presynaptic Ca^{2+} influx at parallel fibre synapses of the rat cerebellum. *J Physiol* **557**, 159–174.

Dodge FA & Rahamimoff R (1967). Co-operative action of calcium ions in transmitter release at the neuromuscular junction. *J Physiol* **193**, 419–432.

Dunnett SB & Fibiger HC (1993). Role of forebrain cholinergic system in learning and memory: relevance to the cognitive deficits of aging and Alzheimer's dementia Prog. *Brain Res* **98**, 413–420.

Eaton MJ, Wagner CK, Moore KE & Lokkingland KJ (1994). Neurochemical identification of A_{13} dopaminergic neuronal projections from the medial zona interna to the horizontal limb of the diagonal band of Broca and the central nucleus of the amygdala. *Brain Res* **659**, 201–207.

Faber DS & Korn H (1991). Application of the coefficient of variation method for analyzing synaptic plasticity. *Biophys J* **60**, 1288–1294.

Fletcher CF, Lutz CM, O'Sullivan TN, Shaughnessy JD Jr, Hawks R, Frankel WN, Copeland NG & Jenkins NA (1996). Absence epilepsy in tottering mutant mice is associated with calcium channel defect. *Cell* **87**, 607–617.

Gaula C & Mesulam MM (1994). Cholinergic systems and related neuropathological predilection patterns in Alzheimer's disease. In *Alzheimer's Disease,* ed. Terry RD, Katzman B & Bic KL, pp. 263–291. Rave Press, New York.

Griffith WH (1988). Membrane properties of cell types within guinea pig basal forebrain nuclei in vitro. *J Neurophysiol* **59**, 1590–1612.

Gritti I, Mainville L, Mancia M & Jones BE (1997). GABAergic and other noncholinergic basal forebrain neurons, together with cholinergic neurons, project to the mesocortex and isocortex in the rat. *J Comp Neurol* **383**, 163–177.

Hartig W, Seeger J, Naumann T, Brauer K & Bruckner G (1998). Selective in vivo fluorescence labelling of cholinergic neurons containing p75 (NTR) in the rat basal forebrain. *Brain Res* **808**, 155–165.

Iwasaki S, Momiyama A, Uchitel OD & Takahashi T (2000). Developmental changes in calcium channel types mediating central synaptic transmission. *J Neurosci* **20**, 59–65.

Jenkinson DH (1957). The nature of the antagonism between calcium and magnesium ions at the neuromuscular junction. *J Physiol* **138**, 434–444.

Kamiya H & Zucker RS (1994). Residual Ca^{2+} and short-term synaptic plasticity. *Nature* **371**, 603–606.

Kebabian JW & Calne DB (1979). Multiple receptors for dopamine. *Nature* **177**, 93–96.

Kimura M, Saitoh N & Takahashi T (2003). Adenosine A_1 receptor-mediated presynaptic inhibition at the calyx of Held of immature rats. *J Physiol* **553**, 415–426.

Kuhnt U & Voronin LL (1994). Interaction between paired-pulse facilitation and long-term potentiation in area CA1 of guinea-pig hippocampal slices: application of quantal analysis. *Neuroscience* **62**, 391–397.

Lezcano N, Myzljac L, Eubanks S, Levenson R & Goldman-Rakic P & Bergson C (2000). Dual signaling regulated by calcyon, a D1dopamine receptor interacting protein. *Science* **287**, 1660–1664.

Luebke JI, Dunlap K & Turner TJ (1993). Multiple calcium channel types control glutamatergic synaptic transmission in the hippocampus. *Neuron* **11**, 895–902.

Manabe T, Wyllie DJ, Perkel DJ & Nicoll RA (1993). Modulation of synaptic transmission and long-term potentiation: effects on paired pulse facilitation and EPSC variance in the CA1 region of the hippocampus. *J Neurophysiol* **70**, 1451–1459.

Mann DMA (1988). Neuropathological and neurochemical aspects of Alzheimer's disease. In *Handbook of Psychopharmacology* , ed. Iversen SD, Iversen LL & Snyder SH, Vol. 22, pp. 1–56. Plenum Press, New York.

Manns ID, Mainville L & Jones BE (2001). Evidence for glutamate, in addition to acetylcholine and GABA, neurotransmitter synthesis in basal forebrain neurons projecting to the entorhinal cortex. *Neuroscience* **107**, 249–263.

Martinez-Murillo R, Semenenko F & Cuello AC (1988). The origin of tyrosine hydroxylase-immunoreactive fibres in the region of the nucleus basalis magnocellularis of the rat. *Brain Res* **451**, 227–236.

Mintz IM, Sabatini BL & Regehr WG (1995). Calcium control of transmitter release at a cerebellar synapse. *Neuron* **15**, 675–688.

Momiyama T (2003). Parallel decrease in ω-conotoxin-sensitive transmission and dopamine-induced inhibition at the striatal synapse of developing rats. *J Physiol* **546**, 483–490.

Momiyama T & Koga E (2001). Dopamine D_2-like receptors selectively block N-type Ca^{2+} channels to reduce GABA release onto rat striatal cholinergic interneurones. *J Physiol* **533**, 479–492.

Momiyama T, Sim JA & Brown DA (1996). Dopamine D_1-like receptor-mediated presynaptic inhibition of excitatory transmission onto rat magnocellular basal forebrain neurones. *J Physiol* **495**, 97–106.

Momiyama T & Zaborszky L (2006). Somatostatin presynaptically inhibits both GABA and glutamate release onto basal forebrain cholinergic neurons. *J Neurophysiol* **96**, 686–694.

Mori Y, Friedrich T, Kim MS, Mikami A, Nakai J, Ruth P, Bosse E, Hofmann F, Flockerzi V, Fruichi T, Mikoshiba K, Imoto K, Tanabe T & Numa S (1991). Primary structure and functional expression from complementary DNA of a brain calcium channel. *Nature* **350**, 398–402.

Muir JL, Everitt BJ & Robbins TW (1994). AMPA-induced excitotoxic lesions of the basal forebrain: a significant role for the cortical cholinergic system in attentional function. *J Neurosci* **14**, 2313–2326.

Neher E (1998). Vesicle pools and Ca^{2+} microdomains: new tools for understanding their roles in neurotransmitter release. *Neuron* **20**, 389–399.

Newcomb R, Szoke B, Palma A, Wang G, Chen X, Hopkins W, Cong R, Miller J, Urge L, Tarczy-Hoenoch K, Loo JA, Dooley DJ, Nadasdi L, Tsien RW, Lemos J & Miljanich G (1998). Selective peptide antagonist of the class E calcium channel from the venom of the tarantula *Hysterocrates gigas*. *Biochemistry* **37**, 15253–15362.

Oyanagi K, Takahashi H, Wakabayashi K & Ikuta F (1989). Correlative decrease of large neurons in the neostriatum and basal nucleus of Meynert in Alzheimer's disease. *Brain Res* **504**, 354–357.

Perry EK, Irving D, Kerwin JM, McKeith IG, Thomson P, Collerton D, Fairbairn AF, Ince PG, Morris CM, Cheng AV & Perry RH (1993). Cholinergic transmitter neurotrophic activities in Lewy body dementia: similarity to Parkinson's and distinction from Alzheimer's disease. *Alz Dis Assoc Disord* **7**, 69–72.

Price DL, Whitehouse PJ & Struble RG (1986). Cellular pathology in Alzheimer's and Parkinson's disease. *Trends Neurosci* **9**, 29–33.

Regehr WG & Mintz IM (1994). Participation of multiple calcium channel types in transmission at single climbing fiber to Purkinje cell synapses. *Neuron* **12**, 605–613.

Reid CA, Bekkers JM & Clements JD (1998). N- and P/Q-type Ca^{2+} channels mediate transmitter release with a similar cooperativity at rat hippocampal autapses. *J Neurosci* **18**, 2849–2855.

Rye DB, Wainer BH, Mesulam M-M, Mufson EJ & Saper CB (1984). A study of cholinergic and noncholinergic components employing combined retrograde tracing and immunohistochemical localization of choline acetyltransferase. *Neuroscience* **13**, 627–643.

Saper CB (1984). Organization of cerebral cortical afferent systems in the rat. II. Magnocellular basal nucleus. *J Comp Neurol* **222**, 313–342.

Sasaki S, Huda K, Inoue T, Miyata M & Imoto K (2006). Impaired feedforward inhibition of the thalamocortical projection in epileptic Ca^{2+} channel mutant mice, tottering. *J Neurosci* **26**, 3056–3065.

Semba K, Reiner PB, McGeer EG & Fibiger HC (1988). Brain stem afferents to the magnocellular basal forebrain studied by axonal transport, immunohistochemistry, and electrophysiology in the rat. *J Comp Neurol* **267**, 433–453.

Sobreviela T, Clary DO, Reichardt LF, Brandabur MM, Kordower JH & Mufson EJ (1994). TrkA-immunoreactive profiles in the central nervous system: colocalization with neurons containing p75 nerve growth factor receptor, choline acetyltransferase, and serotonin. *J Comp Neurol* **350**, 587–611.

Stefani A, Spadoni F & Bernardi G (1998). Group III metabotropic glutamate receptor agonists modulate high voltage-activated Ca^{2+} currents in pyramidal neurons of the adult rat. *Exp Brain Res* **119**, 237–244.

Surmeier DJ, Bargas J, Hemmings HJ, JrNairn AC & Greengard P (1995). Modulation of calcium currents by a D_1 dopaminergic protein kinase/phosphatase cascade in rat neostriatal neurons. *Neuron* **14**, 385–397.

Takahashi T, Forsythe ID, Tsujimoto T, Barnes-Davies M & Onodera K (1996). Presynaptic calcium current modulation by a metabotropic glutamate receptor. *Science* **274**, 594–597.

Takahashi T & Momiyama A (1993). Different types of calcium channels mediate central synaptic transmission. *Nature* **366**, 156–158.

Triggle DJ (2006). L-type calcium channels. *Curr Pharm Des* **12**, 443–457.

Umemiya M & Berger AJ (1994). Activation of adenosine A_1 and A_2 receptors differentially modulates calcium channels and glycinergic synaptic transmission in rat brainstem. *Neuron* **13**, 1439–1446.

Wang G, Dayanithi G, Newcomb R & Lemos JR (1999). An R-type Ca^{2+} current in neurohypophysial terminals preferentially regulates oxytocin secretion. *J Neurosci* **12**, 9235–9241.

Wheeler DB, Randall A & Tsien RW (1994). Roles of N-type and Q-type Ca^{2+} channels in supporting hippocampal synaptic transmission. *Science* **264**, 107–111.

Wu LG, Borst JGG & Sakmann B (1998). R-type Ca^{2+} currents evoke transmitter release at a rat central synapse. *Proc Natl Acad Sci U S A* **95**, 4720–4725.

Wu LG & Saggau P (1994). Pharmacological identification of two types of presynaptic voltage-dependent calcium channels at CA3-CA1 synapses of the hippocampus. *J Neurosci* **14**, 5613–5622.

Wu M, Shanabrough M, Leranth C & Alreja M (2000). Cholinergic excitation of septohippocampal GABA but not cholinergic neurons: Implications for learning and memory. *J Neurosci* **15**, 3900–3908.

Xu W & Lipscombe D (2001). Neuronal $Ca_V1.3\alpha_1$ L-type channels activate at relatively hyperpolarized membrane potentials and are incompletely inhibited by dihydropyridines. *J Neurosci* **21**, 5944–5951.

Zucker RS (1999). Calcium and activity-dependent synaptic plasticity. *Curr Opin Neurobiol* **9**, 305–313.

Acknowledgements

The authors are grateful to K. Matsui, A. Momiyama and J. A. Sim for useful comments and discussion on the data and manuscript, and to T. Kise for technical assistance. This work was supported by a Grant-in-Aid for Scientific Research from the Ministry of Education, Culture, Sports, Science and Technology of Japan (no. 15016106, 15500292 and 16015314), and Core Research for Evolutional Science and Technology (CREST) from Japan Science and Technology Corporation.